

ACKNOWLEDGEMENTS

The author wishes to express her thanks to Dr. A.M. El-Serafi for his guidance, encouragement and interest in this project. His provocative discussions, invaluable assistance and many hours of patience in the preparation of the text of this thesis is especially acknowledged.

The author wishes to extend her thanks to the members of the Advisory Committee for their helpful discussion at various times during the course of this work. She is also grateful to Professor A.E. Krause for his patience and help in the work conducted on the PDP LAB-8/E minicomputer.

Acknowledgement is due to Messers J. Yourk and V. Meyers for their continuous help during the experimental work; to Mr. G. Dyck and the staff of the central shop for providing the necessary adjustment of the microalternator set; to Mrs. A. Johnston for her prompt and accurate typing of the manuscript.

Gratitude is expressed to both Ain Shams University (Cairo-Egypt) for granting leave and permission to pursue postgraduate studies in Canada, and to the University of Saskatchewan for a scholarship received during this project. Acknowledgement is also given to the financial support of the National Research Council of Canada under grant No. A7115.

Finally, the author wishes to take this opportunity to express her thanks to her husband Hamdy, for his invaluable assistance in the preparation of the manuscript.

UNIVERSITY OF SASKATCHEWAN

Electrical Engineering Abstract #80A208

THEORETICAL AND EXPERIMENTAL INVESTIGATIONS ON THE PERFORMANCE
OF SYNCHRONOUS MACHINES UNDER THYRISTOR-BRIDGE LOAD OPERATION

Student: Somaya A. Shehata Supervisor: Ahmed M. El-Serafi

Ph.D. Thesis presented to the College of Graduate Studies and Research

September 1980

ABSTRACT

In recent years, the level of harmonics in power systems has become relatively high. Meantime, there is a tendency to eliminate the filters which are usually provided to absorb these harmonics. This has triggered an interest for investigating the interaction between synchronous generators and thyristor-bridge loads and for studying the effect of the harmonics on the performance of synchronous machines.

In this thesis, a rigorous and an easily manipulated analysis has been developed for the determination of the performance of synchronous generators supplying thyristor-bridge loads. This analysis accounts for the full interaction between the synchronous generator and the thyristor-bridge load. The developed analysis is capable of predicting the waveforms of the various variables of the synchronous generator, and their harmonic contents for two cases: (i) when the resistances are neglected, and (ii) when the resistances are taken into consideration. The algorithm of solution of this analysis avoids the use of an iteration process when the resistances are neglected.

Special considerations have been given in this thesis to the design features of synchronous generators supplying thyristor-bridge loads. In this regard, a great deal of work was devoted to the investigation of the effect of the synchronous machine parameters and the system operating conditions on the harmonic levels of its various variables as well as on the copper losses in the machine windings. The findings of these studies would provide the guide lines for designing synchronous machines to cope with the thyristor-bridge loading.

In order to examine the validity of the analysis, extensive experimental investigations were carried out on a microalternator supplying a thyristor-bridge load. In these investigations, the PDP LAB-8/E minicomputer has been used for acquiring, storing and processing the experimental results. The studies have been conducted for different operating conditions as well as for various external inductances and resistances inserted in the microalternator circuits. The comparison made between the experimental and analytical results has proved the general validity of the analysis.

The author has agreed that the Library, University of Saskatchewan, shall make this thesis freely available for inspection. Moreover, the author has agreed that permission for extensive copying of this thesis for scholarly purposes may be granted by the professor or professors who supervised the thesis work recorded herein or, in their absence, by the Head of the Department or the Dean of the College in which the thesis work was done. It is understood that due recognition will be given to the author of this thesis and to the University of Saskatchewan in any use of material in this thesis. Copying or publication or any other use of the thesis for financial gain without approval by the University of Saskatchewan and the author's written permission is prohibited.

Requests for permission to copy or to make other use of material in this thesis in whole or in part should be addressed to:

Head of the Department of Electrical Engineering

University of Saskatchewan

Saskatoon, Canada

TABLE OF CONTENTS

	Page
COPYRIGHT	ii
ACKNOWLEDGEMENTS	iii
ABSTRACT	iv
TABLE OF CONTENTS	v
LIST OF FIGURES	ix
LIST OF TABLES	xvii
LIST OF SYMBOLS	xix
1. <u>INTRODUCTION</u>	1
1.1 General	1
1.2 Effect of Harmonics on the Performance of Synchronous Machines	2
1.3 Effect of Synchronous Machine Parameters on the Harmonics	6
1.4 Purpose of the Thesis	7
2. <u>ANALYSIS OF SYNCHRONOUS MACHINES WITH THYRISTOR-BRIDGE LOADS</u>	10
2.1 General	10
2.2 Mathematical Model of the System	10
2.2.1 Synchronous generator equations	10
2.2.1.1 Flux linkage equations	12
2.2.1.2 Voltage equations	14
2.2.1.3 Torque equation	14
2.2.2 Transformer equations	14
2.2.3 Thyristor-bridge circuit representation	14
2.2.4 Combined model of the system	16
2.3 System Performance Equations Neglecting Resistances	17
2.3.1 Commutation interval equations	18
2.3.1.1 Torque equation	23
2.3.2 Commutation angle equation	23
2.3.3 Interlude interval equations	24
2.3.3.1 Torque equation	26
2.3.4 Displacement angle equation	26

THEORETICAL AND EXPERIMENTAL INVESTIGATIONS
ON THE PERFORMANCE OF SYNCHRONOUS
MACHINES UNDER THYRISTOR-BRIDGE LOAD OPERATION

A Thesis

Submitted to the Faculty of Graduate Studies and Research
in Partial Fulfilment of the Requirements
for the Degree of
Doctor of Philosophy
in the Department of Electrical Engineering
University of Saskatchewan

by

Somaya Afify M. Shehata

Saskatoon, Saskatchewan

September, 1980

The author claims copyright. Use shall not be made of the material contained herein without proper acknowledgement, as indicated on the following page.

TABLE OF CONTENTS (Continued)

	Page
2.3.5 Generalized form of the system equations	29
2.3.6 Terminal voltage equations	31
2.3.7 Average output DC voltage	33
2.4 Method of Computation Neglecting Resistances	39
2.4.1 Calculation of the displacement angle, the commutation angle and the values of the initial rotor currents	39
2.4.2 Digital simulation	40
2.5 System Performance Equations Considering Resistances	43
2.5.1 Commutation interval equations	43
2.5.1.1 Torque equation	47
2.5.2 Commutation angle equation	47
2.5.3 Interlude interval equations	47
2.5.3.1 Torque equation	48
2.5.4 Displacement angle equation	48
2.5.5 Generalized form of the system equations	50
2.5.6 Machine terminal voltage equations	51
2.6 Method of Computation Considering Resistances	54
2.7 Summary	59
3. <u>EFFECT OF SYNCHRONOUS GENERATORS OPERATING CONDITIONS AND PARAMETERS ON THEIR PERFORMANCE UNDER THYRISTOR-BRIDGE OPERATION</u>	63
3.1 General	63
3.2 System Operating Conditions	63
3.3 Harmonic Analysis of the System Variables	64
3.4 Effect of System Operating Conditions	70
3.4.1 Effect of firing delay angle	70
3.4.2 Effect of output DC current	74
3.5 Effect of Machine Parameters	79
3.5.1 Effect of magnetizing inductances	79
3.5.2 Effect of armature winding leakage inductance	85
3.5.3 Effect of rotor leakage inductances	92
3.5.4 Effect of subtransient saliency	99
3.5.5 Effect of the machine resistances	103
3.6 Summary	115
4. <u>ADDITIONAL LOSSES OF SYNCHRONOUS MACHINES UNDER THYRISTOR-BRIDGE OPERATION</u>	116

TABLE OF CONTENTS (Continued)

	Page
6. <u>EXPERIMENTAL INVESTIGATIONS - RESULTS</u>	172
6.1 General	172
6.2 Test Operating Conditions	172
6.3 Experimental Studies Under Normal Operating Conditions	176
6.4 Experimental Studies With Various Operating Conditions and Machine Parameters	189
6.4.1 Test results for various operating conditions	190
6.4.1.1 Variation of firing delay angle	190
6.4.1.2 Variation of DC load current	199
6.4.2 Variation of the machine leakage inductances	207
6.4.3 Variation of the d- and q-axis damper winding resistances	223
6.5 Discussions	238
6.6 Summary	253
7. <u>SUMMARY AND CONCLUSIONS</u>	255
7.1 General	255
7.2 Theoretical Studies	255
7.3 Experimental Studies	259
7.4 Recommended Design Features of Synchronous Generators With Thyristor-Bridge Loads	262
8. <u>REFERENCES</u>	264
9. <u>APPENDICES</u>	271
A. Per-Unit System of Synchronous Machines	271
B. Expressions of the Average Rotor Currents	278
C. Solution of Nonlinear Algebraic Equations by Newton Raphson Method	301
D. Per-Unit System of the AC/DC System	336
E. System Data in p.u.	339
F. Calculation of the Stator and Rotor Base Values	340

LIST OF FIGURES

Figure		Page
1.1	Generation of Harmonic Currents of Order $6k$ in the Rotor	3
2.1	System Under Investigation	11
2.2	Schematic Diagram of a Synchronous Machine	11
2.3	Different Modes of Operation of the Thyristor-Bridge	15
2.4	Simplified Flow Chart for the Algorithm of Computation When the Resistances are Neglected	45
2.5	Integration Procedure for Calculating the Machine Variables	56
2.6	Simplified Flow Chart for the Algorithm of Computation When the Resistances are Considered	61
3.1	Waveforms of Various Variables of Synchronous Machine Under Normal Operating Conditions (a) v_3 (b) i_c (c) i_f (d) i_{kd} (e) i_{kq} (f) T_E	66
3.2	Frequency Spectrum of Various Variables of Synchronous Machine Under Normal Operating Conditions (a) v_3 (b) i_c (c) i_f (d) i_{kd} (e) i_{kq} (f) T_E	68
3.3	Effect of the Variation of α from 0° to 60° on the Waveforms of: (a) v_3 (b) i_c (c) i_f (d) i_{kd} (e) i_{kq} (f) T_E	71
3.4	Effect of the Variation of α from 0° to 60° in Steps of 10° on the Harmonic Components of: (a) v_3 (b) i_c (c) i_f (d) i_{kd} (e) i_{kq} (f) T_E	73
3.5	Effect of the Variation of I from 0.1 p.u. to 1.0 p.u. on the Waveforms of: (a) v_3 (b) i_c (c) i_f (d) i_{kd} (e) i_{kq} (f) T_E	75
3.6	Effect of the Variation of I from 0.2 p.u. to 1.0 p.u. in Steps of 0.2 p.u. on the Harmonic Components of: (a) v_3 (b) i_c (c) i_f (d) i_{kd} (e) i_{kq} (f) T_E	77

LIST OF FIGURES (Continued)

Figure		Page
3.7	Effect of the Variation of I from 0.2 p.u. to 1.0 p.u. in Steps of 0.2 p.u. on the Absolute Values of the Harmonic Components of: (a) i_c (b) T_E	78
3.8	Effect of the Variation of L_{ad} from 0.7 p.u. to 1.3 p.u. on the Waveforms of: (a) v_3 (b) i_c (c) i_f (d) i_{kd} (e) i_{kq} (f) T_E	80
3.9	Effect of the Variation of L_{ad} from 0.7 p.u. to 1.3 p.u. in Steps of 0.1 p.u. on the Absolute Values of the Harmonic Components of: (a) v_3 (b) i_c (c) i_f (d) i_{kd} (e) i_{kq} (f) T_E	82
3.10	Effect of the Variation of L_{ad}° from 0.7 p.u. to 1.3 p.u. in Steps of 0.1 p.u. on the Harmonic Analysis of: (a) v_3 (b) i_c (c) i_f (d) i_{kd} (e) i_{kq} (f) T_E	84
3.11	Effect of the Variation of L_{aq} from 0.236 p.u. to 0.836 p.u. on the Waveforms of: (a) v_3 (b) i_c (c) i_f (d) i_{kd} (e) i_{kq} (f) T_E	86
3.12	Effect of the Variation of L_{aq} from 0.236 p.u. to 0.836 p.u. in Steps of 0.1 p.u. on the Harmonic Components of: (a) v_3 (b) i_c (c) i_f (d) i_{kd} (e) i_{kq} (f) T_E	88
3.13	Effect of the Variation of L_{al} from 0.03 p.u. to 0.18 p.u. on the Waveforms of: (a) v_3 (b) i_c (c) i_f (d) i_{kd} (e) i_{kq} (f) T_E	89
3.14	Effect of the Variation of L_{al} from 0.03 p.u. to 0.18 p.u. in Steps of 0.03 p.u. on the Harmonic Components of: (a) v_3 (b) i_c (c) i_f (d) i_{kd} (e) i_{kq} (f) T_E	91
3.15	Effect of the Variation of L_{fl} from 0.12 p.u. to 0.36 p.u. on the Waveforms of: (a) v_3 (b) i_c (c) i_f (d) i_{kd} (e) i_{kq} (f) T_E	93
3.16	Effect of the Variation of L_{fl} from 0.06 p.u. to 0.42 p.u. in Steps of 0.06 p.u. on the Harmonic Components of: (a) v_3 (b) i_c (c) i_f (d) i_{kd} (e) i_{kq} (f) T_E	95

LIST OF FIGURES (Continued)

Figure		Page
3.17	Effect of the Variation of $L_{kd\ell}$ from 0.1 p.u. to 0.7 p.u. on the Waveforms of: (a) v_3 (b) i_c (c) i_f (d) i_{kd} (e) i_{kq} (f) T_E	96
3.18	Effect of the Variation of $L_{kd\ell}$ from 0.1 p.u. to 0.7 p.u. in Steps of 0.1 p.u. on the Harmonic Components of: (a) v_3 (b) i_c (c) i_f (d) i_{kd} (e) i_{kq} (f) T_E	98
3.19	Effect of the Variation of $L_{kq\ell}$ from 0.0536 to 0.3216 p.u. on the Waveforms of: (a) v_3 (b) i_c (c) i_f (d) i_{kd} (e) i_{kq} (f) T_E	100
3.20	Effect of the Variation of $L_{kq\ell}$ from 0.0536 p.u. to 0.3216 p.u. in Steps of 0.0536 p.u. on the Harmonic Components of: (a) v_3 (b) i_c (c) i_f (d) i_{kd} (e) i_{kq} (f) T_E	102
3.21	Effect of the Subtransient Saliency on the Disturbances of the Voltage Waveform	104
3.22	Effect of the Synchronous Machine Resistances, at a Speed 1.0 p.u., on the Harmonic Components of: (a) v_3 (b) i_c (c) i_f (d) i_{kd} (e) i_{kq} (f) T_E	107
3.23	Effect of the Synchronous Machine Resistances, at a Speed of 0.5 p.u., on the Harmonic Components of: (a) v_3 (b) i_c (c) i_f (d) i_{kd} (e) i_{kq} (f) T_E	110
3.24	Effect of the Synchronous Machine Resistances, at a speed of 0.2 p.u., on the Harmonic Components of: (a) v_3 (b) i_c (c) i_f (d) i_{kd} (e) i_{kq} (f) T_E	112
3.25	Effect of the Variation of the Resistances, at a Speed of 0.2 p.u., on the Waveforms of: (a) v_3 (b) i_c (c) i_f (d) i_{kd} (e) i_{kq} (f) T_E	114
4.1	Effect of the Firing Delay Angle α on the Machine Losses	122
4.2	Effect of the Output DC Current I on the Machine Losses	123
4.3	Effect of the d-axis Magnetizing Inductance L_{ad} on the Machine Losses	125
4.4	Effect of the q-axis Magnetizing Inductance L_{aq} on the Machine Losses	127

LIST OF FIGURES (Continued)

Figures		Page
4.5	Effect of the Armature Winding Leakage Inductance L_{al} on the Machine Losses	128
4.6	Effect of the Field Winding Leakage Inductance L_{fl} on the Machine Losses	129
4.7	Effect of the q-axis Damper Winding Leakage Inductance $L'_{kq\ell}$ on the Machine Losses	131
4.8	Effect of the d-axis Damper Winding Leakage Inductance $L'_{kd\ell}$ on the Machine Losses	132
5.1	Schematic Diagram of the Experimental Set Up	135
5.2	Photograph of the System Used for Experimental Investigations	136
5.3	DC Motor-Generator Set for Supplying the Excitation Winding of the Microalternator	138
5.4	DC V-I Characteristic of the Armature Winding	139
5.5	DC V-I Characteristics of the Rotor Windings	139
5.6	The Open-Circuit, Short-Circuit and Zero Power Factor Characteristics in the D-axis	141
5.7	The Open-Circuit and Short-Circuit Characteristics in the Q-axis	142
5.8	Oscillograms of the Microalternator Currents	144
5.9	(a) Transient and Subtransient Components of the Short-Circuit Armature Current (b) Subtransient Component of the Short-Circuit Armature Current	145
5.10	The 3-Phase Thyristor-Bridge Load	148
5.11	(a) Schematic Diagram of the Phase Shifting Circuit (b) Vector Diagram of the Phase Shifting Circuit	148
5.12	Open-Circuit Gate Voltage Shown at 180° Conduction Angle	150
5.13	Gate Pulse Phase Angle With Control Signal	150
5.14	Terminals of the 3-Phase Firing Circuit	150
5.15	Thyristor-Bridge Load: (a) Front View, (b) Back View	152

LIST OF FIGURES (Continued)

Figure		Page
5.16	Circuit Diagram of the Current Transducer "TransfoSHUNT"	154
5.17	Current Transducer Connection With Off-Set Compensation	154
5.18	Basic Construction of the Coaxial Coil System	158
5.19	Schematic Diagram for Torque Measurement	159
5.20	Schematic Diagram for the Measurement of the Displacement Angle	160
5.21	PDP LAB-8/E Minicomputer	161
5.22	(a) Amplitude Response of the Analog filters (b) Phase Shift Response of the Analog filters	163
5.23	Flow Chart of Data Acquisition Software	165
5.24	Illustration of the Method of Determining the Instant at Which the Wave Amplitude is Equal to the Amplitude of Sample #1	169
6.1	Oscillograms of: (1) Terminal Voltage, (2) Armature Current, (3) Field Current, (4) D-axis Damper Winding Current, (5) Q-axis Damper Winding Current	174
6.2	Measurement of Firing Delay Angle α and Commutation Angle γ From Oscillograms of Machine Voltage	175
6.3	Waveforms of Microalternator Variables Under Normal Operating Conditions: (a) Armature Current, (b) Terminal Voltage, (c) Field Current, (d) D-axis Damper Current, (e) Q-axis Damper Current, (f) Electromagnetic Torque	179
6.4	(a) Bridge Circuit (b) Rectifier Current Waveform ($\alpha = 0^\circ$)	180
6.5	Waveforms of the Microalternator No Load Voltage	182
6.6	(a) Bridge Circuit (b) Voltage Waveforms (c) Armature Current Waveform (d) Armature Current Derivative ($\alpha = 10^\circ$)	184
6.7	Frequency Spectrum of Various Microalternator Variables With Nominal Data and Under Normal Operating Conditions (a) Armature Current, (b) Terminal Voltage, (c) Field Current, (d) D-axis Damper Current, (e) Q-axis Damper Current, (f) Electromagnetic Torque	187

LIST OF FIGURES (Continued)

Figure		Page
6.8	Waveforms of Microalternator Variables for $\alpha = 50^\circ$ (a) Terminal Voltage, (b) Armature Current, (c) Field Current, (d) D-axis Damper Current, (e) Q-axis Damper Current, (f) Electromagnetic Torque	193
6.9	Effect of the Variation of α from 0° to 50° on the Harmonic Components of: (a) Terminal Voltage, (b) Armature Current, (c) Field Current, (d) D-axis Damper Current, (e) Q-axis Damper Current, (f) Electromagnetic Torque Case 1: $\alpha = 0^\circ$ Case 2: $\alpha = 10^\circ$ Case 3: $\alpha = 20^\circ$ Case 4: $\alpha = 30^\circ$ Case 5: $\alpha = 40^\circ$ Case 6: $\alpha = 50^\circ$	196
6.10	Waveforms of Microalternator Variables for $I = 0.38$ p.u. (a) Terminal Voltage, (b) Armature Current, (c) Field Current, (d) D-axis Damper Current, (e) Q-axis Damper Current, (f) Electromagnetic Torque	202
6.11	Effect of the Variation of I on the Harmonic Components of: (a) Terminal Voltage, (b) Armature Current, (c) Field Current, (d) D-axis Damper Current, (e) Q-axis Damper Current, (f) Electromagnetic Torque	204
6.12	Waveforms of Microalternator Variables for $L_{ae} = 0.12416$ p.u. (a) Terminal Voltage, (b) Armature Current, (c) Field Current, (d) D-axis Damper Current, (e) Q-axis Damper Current, (f) Electromagnetic Torque	210
6.13	Effect of the Variation of L_{ae} on the Harmonic Components of: (a) Terminal Voltage, (b) Armature Current, (c) Field Current, (d) D-axis Damper Current, (e) Q-axis Damper Current, (f) Electromagnetic Torque Case 1: $L_{ae} = 0.0$ p.u. Case 2: $L_{ae} = 0.0535$ p.u. Case 3: $L_{ae} = 0.0806$ p.u. Case 4: $L_{ae} = 0.12415$ p.u.	212
6.14	Waveforms of Microalternator Variables for $L_{fe} = 0.2243$ p.u. (a) Terminal Voltage, (b) Armature Current, (c) Field Current, (d) D-axis Damper Current, (e) Q-axis Damper Current, (f) Electromagnetic Torque	218
6.15	Effect of the Variation of L_{fe} on the Harmonic Components of: (a) Terminal Voltage, (b) Armature Current, (c) Field Current, (d) D-axis Damper Current, (e) Q-axis Damper Current, (f) Electromagnetic Torque Case 1: $L_{fe} = 0.0$ p.u. Case 2: $L_{fe} = 0.02553$ p.u. Case 3: $L_{fe} = 0.0546$ p.u. Case 4: $L_{fe} = 0.082$ p.u. Case 5: $L_{fe} = 0.4474$ p.u. Case 6: $L_{fe} = 0.14265$ p.u. Case 7: $L_{fe} = 0.2243$ p.u.	220

LIST OF FIGURES (Continued)

Figure		Page
6.16	Waveforms of Microalternator Variables for $L_{kde} = 0.1154$ p.u. (a) Terminal Voltage, (b) Armature Current, (c) Field Current, (d) D-axis Damper Current, (e) Q-axis Damper Current, (f) Electromagnetic Torque	226
6.17	Effect of the Variation of L_{kde} on the Harmonic Components of: (a) Terminal Voltage, (b) Armature Current (c) Field Current, (d) D-axis Damper Current, (e) Q-axis Damper Current, (f) Electromagnetic Torque Case 1: $L_{kde} = 0.0$ p.u. Case 2: $L_{kde} = 0.0197$ p.u. Case 3: $L_{kde} = 0.0392$ p.u. Case 4: $L_{kde} = 0.0564$ p.u. Case 5: $L_{kde} = 0.0795$ p.u. Case 6: $L_{kde} = 0.1154$ p.u.	228
6.18	Waveforms of Microalternator Variables for $L_{kqe} = 0.32554$ p.u. (a) Terminal Voltage, (b) Armature Current, (c) Field Current, (d) D-axis Damper Current, (e) Q-axis Damper Current, (f) Electromagnetic Torque	233
6.19	Effect of the Variation of L_{kqe} on the Harmonic Components of: (a) Terminal Voltage, (b) Armature Current, (c) Field Current, (d) D-axis Damper Current, (e) Q-axis Damper Current, (f) Electromagnetic Torque Case 1: $L_{kqe} = 0.0$ p.u. Case 2: $L_{kqe} = 0.0463$ p.u. Case 3: $L_{kqe} = 0.0927$ p.u. Case 4: $L_{kqe} = 0.1375$ p.u. Case 5: $L_{kqe} = 0.2299$ p.u. Case 6: $L_{kqe} = 0.3255$ p.u.	235
6.20	Waveforms of Microalternator Variables for $R_{kde} = 2.58$ p.u. and $R_{kqe} = 2.776$ p.u. (a) Terminal Voltage, (b) Armature Current, (c) Field Current, (d) D-axis Damper Current, (e) Q-axis Damper Current, (f) Electromagnetic Torque	242
6.21	Effect of the Variation of R_{kde} and R_{kqe} on the Harmonic Components of: (a) Terminal Voltage, (b) Armature Current, (c) Field Current, (d) D-axis Damper Current, (e) Q-axis Damper Current, (f) Electromagnetic Torque Case 1: $R_{kde} = 0.0$ p.u., $R_{kqe} = 0.0$ p.u. Case 2: $R_{kde} = 1.141$ p.u., $R_{kqe} = 1.236$ p.u. Case 3: $R_{kde} = 2.58$ p.u., $R_{kqe} = 2.776$ p.u.	244
9.1	(a) No Load Air-Gap Flux Plot in Which the Excitation is Provided by the Field MMF (b) Approximation to the Air-Gap Variation Over Bevelled Region of Pole	343
9.2	(a) Air-Gap Flux Plot Due to the Sinusoidal MMF of a Unit Stator Current Acting on the Direct-Axis (b) Approximation to the Air-Gap Over Bevelled Region of Pole	344

LIST OF FIGURES (Continued)

Figure		Page
9.3	(a) Air-Gap Flux Plot Due to the Sinusoidal MMF of a Unit Stator Current Acting on the Quadrature-Axis (b) Approximation to the Air-Gap Over Bevelled Region of Pole	345
9.4	(a) Air-Gap Flux Plot Due to an MMF of Unit Damper Winding Current Acting on the Quadrature-Axis (b) Approximation to the Air-Gap Over Bevelled Region of Pole	346
9.5	Dimensions of Rotor #4	347

LIST OF TABLES

Table		Page
2.1	Current and Voltage Conditions of the Thyristor-Bridge	17
3.1	The Normal Operating Conditions of the System Under Study (All value are given in per-unit)	65
3.2	Relationship Between Machine Speed, Period of Commutation and Machine Subtransient Time-Constants	108
5.1	Parameters of the Microalternator	147
5.2	Turns Ratio of the Current Transducers "TransfoSHUNTS"	155
6.1	Comparison Between Measured and Calculated Harmonic Spectra of the Normal Case	188
6.2	Comparison Between Measured and Calculated Results For Various Values of α	197
6.3	Comparison Between Measured and Calculated Harmonic Spectra For $\alpha = 50^\circ$	198
6.4	Comparison Between Measured and Calculated Results For Various Values of I	205
6.5	Comparison Between Measured and Calculated Harmonic Spectra for I = 0.38 p.u.	206
6.6	Comparison Between Measured and Calculated Results For Various Values of the External Inductance L_{ae}	213
6.7	Comparison Between Measured and Calculated Harmonic Spectra For $L_{ae} = 0.12415$ p.u. ($1.514 \times L_{al}$)	214
6.8	Comparison Between Measured and Calculated Results For Various Values of the External Inductance L_{fe}	221
6.9	Comparison Between Measured and Calculated Harmonic Spectra For $L_{fe} = 0.2243$ p.u. ($0.8728 \times L_{fl}$)	222
6.10	Comparison Between Measured and Calculated Results For Various Values of the External Inductance L_{kde}	229
6.11	Comparison Between Measured and Calculated Harmonic Spectra for $L_{kde} = 0.1154$ p.u. ($0.6238 \times L_{kdl}$)	230
6.12	Comparison Between Measured and Calculated Results For Various Values of the External Inductance L_{kqe}	236

LIST OF TABLES (Continued)

Table		Page
6.13	Comparison Between Measured and Calculated Harmonic Spectra for $L_{kqe} = 0.32554$ p.u. ($1.102 \times L_{kq\ell}$)	237
6.14	Effect of Varying the D- and Q-Axis Damper Winding Resistances on the Period of Commutation and Machine Subtransient Time-Constants	239
6.15	Comparison Between Measured and Calculated Results For Various Values of the External Resistances R_{kde} and R_{kqe}	245
6.16	Comparison Between Measured and Calculated Harmonic Spectra for $R_{kde} = 2.58$ p.u. ($44.62 \times R_{kd}$) and $R_{kqe} = 2.776$ p.u. ($53.18 \times R_{kq}$)	246
9.1	Design Data of the Microalternator With Rotor #4	353

LIST OF SYMBOLS

a	$\frac{L''_d - L''_q}{L''_d}$
C_o	shift angle
f	frequency
f_1	fundamental frequency
H	step of integration
I	output DC current
[I]	vector of synchronous machine currents
\bar{I}_f	average field current
$\bar{I}_{kd}, \bar{I}_{kq}$	average d- and q-axis damper winding current respectively
\hat{I}_{a_n}	peak value of the nth order harmonic component of the armature current
\hat{I}_{f_n}	peak value of the nth order harmonic component of the field current
$\hat{I}_{kd_n}, \hat{I}_{kq_n}$	peak value of the nth order harmonic component of the d- and q-axis damper winding current respectively
$\bar{I}_{kd_{eq}}, \bar{I}_{kq_{eq}}$	equivalent value of the d- and q-axis damper winding current respectively. $\bar{I}_{kd_{eq}} = \sqrt{(R_f/R_{kd})} \bar{I}_f, \quad \bar{I}_{kq_{eq}} = \sqrt{(R_f/R_{kq})} \bar{I}_f$
i	transient commutation current
i_a, i_b, i_c	3-ph armature current
i_f	field winding current
i_{kd}, i_{kq}	d- and q-axis damper winding current respectively
i_{fo}	field winding current at the start of the commutation interval
i_{kdo}, i_{kqo}	d- and q-axis damper winding current at the start of the commutation interval respectively

LIST OF SYMBOLS (Continued)

$i_{f\gamma}$	field winding current at the end of the commutation interval
$i_{kd\gamma}, i_{kq\gamma}$	d- and q-axis damper winding current at the end of the commutation interval respectively
$i_{f(\pi/3-\alpha)}$	field winding current at $\omega t = \pi/3 - \alpha$
$i_{kd(\pi/3-\alpha)}, i_{kq(\pi/3-\alpha)}$	d- and q-axis damper winding current at $\omega t = \pi/3 - \alpha$ respectively
$i_{f(\pi/3)}$	field winding current at $\omega t = \pi/3$
$i_{kd(\pi/3)}, i_{kq(\pi/3)}$	d- and q-axis damper winding current at $\omega t = \pi/3$ respectively
[L]	synchronous machine inductance matrix
L_{aao}	average value of the stator self-inductance
L_{aa2}	difference between maximum and average value of the stator self-inductance
L_{abo}	average value of the stator mutual inductance
L_{ad}, L_{aq}	d- and q-axis magnetizing inductance respectively
L_{ae}	external inductance inserted in the armature circuit
L_{afdo}	maximum mutual-inductance between field winding and phase a of the stator
L_{akdo}	maximum mutual-inductance between d-axis damper winding and phase a of the stator
L_{akqo}	maximum mutual-inductance between q-axis damper winding and phase a of the stator
L_{al}	armature winding leakage inductance
L_d, L_q	d- and q-axis synchronous inductance respectively
L'_d	d-axis transient inductance
L''_d, L''_q	d- and q-axis subtransient inductance respectively
L_{fdkd}	mutual-inductance between d-axis damper winding and field winding

LIST OF SYMBOLS (Continued)

L_{fe}	external inductance inserted in the field winding
L_{ffd}	self-inductance of the field winding
L_{fl}	field winding leakage inductance
L_{kde}, L_{kqe}	external inductance inserted in the d- and q-axis damper circuit respectively
L_{kdl}, L_{kql}	d- and q-axis damper winding leakage inductance respectively
L_{kkd}, L_{kkq}	d- and q-axis damper winding self-inductance respectively
L_t	transformer leakage inductance
N	$\frac{L_{ad}L_{kkd} - L_{ad}^2}{L_{ffd}L_{kkd} - L_{ad}^2}$
N_c	number of channels
N_{fdl}	field winding effective number of turns
N_{kdl}, N_{kql}	d- and q-axis damper winding effective number of turns respectively
N_s	number of samples per cycle
N_{sl}	stator effective number of turns per phase
n	order of harmonic
P	$\frac{L_{aq}}{L_{kkq}}$
p	$\frac{d}{dt}$
Q	$\frac{L_{ad}L_{ffd} - L_{ad}^2}{L_{ffd}L_{kkd} - L_{ad}^2}$
[R]	synchronous machine resistance matrix
R_a	armature winding resistance
R_f	field winding resistance
R_{kd}, R_{kq}	d- and q-axis damper winding resistances respectively

LIST OF SYMBOLS (Continued)

R_{kde}, R_{kqe}	external resistance inserted in the d- and q-axis damper circuit respectively
R_t	transformer winding resistance
S	sampling frequency
T_E	electromagnetic developed torque
\bar{T}_E	average value of electromagnetic developed torque
\hat{T}_{E_n}	peak value of the nth order harmonic component of the electromagnetic developed torque
t	time in p.u.
$[V]$	vector of machine terminal voltage
\hat{V}_1	peak value of fundamental component of machine terminal voltage
\hat{V}_n	peak value of nth order harmonic component of machine terminal voltage
v_1, v_2, v_3	3-ph machine terminal voltage
v_a, v_b, v_c	3-ph voltage applied to thyristor-bridge
v_f	voltage of field winding
V_f	$\bar{I}_f \times R_f$
v_{kd}, v_{kq}	d- and q-axis damper winding voltage respectively
\bar{v}_{DC}	average value of output DC voltage
x_d, x_q	d- and q-axis synchronous reactance respectively
x'_d	d-axis transient reactance
x''_d, x''_q	d- and q-axis subtransient reactance respectively
$x_{f\ell}$	field winding leakage reactance
x_{kdl}, x_{kql}	d- and q-axis damper winding leakage reactance respectively
x_p	potier reactance

LIST OF SYMBOLS (Continued)

$[\psi]$	vector of synchronous machine flux linkage
ψ_a, ψ_b, ψ_c	3-ph armature flux linkage
ψ_f	field winding flux linkage
ψ_{kd}, ψ_{kq}	d- and q-axis damper winding flux linkage respectively
θ	rotor position with respect to phase a
ϕ_{V1}	phase angle of the fundamental component of machine terminal voltage measured from the reference axis
ϕ_{I1}	phase angle of the fundamental component of the armature current measured from the reference axis
ϕ_1	$=\phi_{V1} - \phi_{I1}$
α	firing delay angle
δ	displacement angle
γ	commutation angle
ω	rotor speed
λ_d, λ_q	d- and q-axis equivalent permeance of the synchronous machine respectively
μ_0	permeability of space

1. INTRODUCTION

1.1 General

In the past, little attention was paid to the effect of the presence of harmonics on the operation of electrical power systems. This is because harmonic levels, in general, were found to be acceptably low. In recent years, however, the level of harmonics in power systems has become relatively high due to the use of high power converters for HVDC transmission systems¹⁻⁴ and the rapidly increasing applications⁵⁻¹⁰ of semiconductor devices, e.g., in static excitation systems,^{11,12} motor speed control,¹³⁻¹⁶ ... etc.

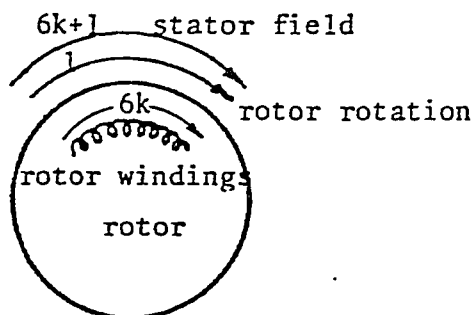
Whenever harmonics are present in high percentage, filter networks are provided to absorb them. However, these filters are relatively expensive (for example, the cost of filters in a HVDC converter station can reach up to 15% of the converter station cost) and their provision introduces many problems.^{3,4} Accordingly, there is a tendency to eliminate these filters especially from systems consisting of isolated generators supplying thyristor-bridge loads, such as AC exciter systems^{11,12} and unit-connection HVDC transmission schemes.¹⁷⁻¹⁹ This has triggered an interest in investigating the interaction between synchronous generators and thyristor-bridge loads when the filters are eliminated, and to examine the effect of the generated harmonic currents on the performance of synchronous machines.

1.2 Effect of Harmonics on the Performance of Synchronous Machines

In all the systems which consist of synchronous generators supplying thyristor-bridge loads, harmonic currents of order $6k \pm 1$ (where k is an integer) are generated^{1,2} by the thyristor-bridge. The flow of these currents in the stator windings of synchronous machines results in harmonic currents of order $6k$ in the rotor windings.²⁰⁻²³ This is because the stator harmonic current of order $6k+1$ (e.g., 7) creates an MMF with the same sense of rotation as that of the rotor, Fig. 1.1a. Therefore, the relative velocity of such an MMF with respect to the rotor is $6k$ times that of the rotor. On the other hand, the corresponding harmonic component of the stator phase currents of order $6k-1$ (e.g., 5) creates an MMF which has also a relative velocity with respect to the rotor of the same value as that of the $6k+1$ harmonic current but of opposite direction, Fig. 1.1b. These two MMFs rotating in opposite directions result in an elliptical field, Fig. 1.1c, and they induce harmonic currents of order $6k$ (e.g., 6) in the rotor surface and windings. In such a case, the rotor circuits will be carrying AC currents even under steady-state conditions.

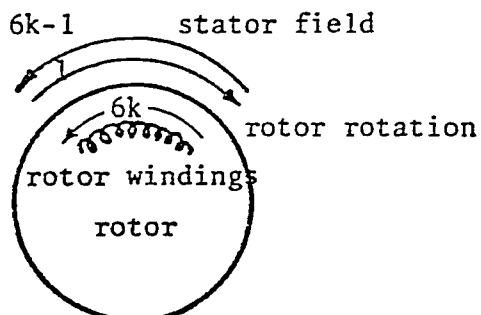
The flow of these harmonic frequency currents in the synchronous machine windings results in the distortion of the waveform of the machine terminal voltage. Such a distortion is unacceptable if the synchronous generator is supplying a load which is sensitive to harmonic voltages.

Moreover, the resultant harmonic rotating air-gap fluxes will interact with the harmonic currents of the machine and results in the production of pulsating electromagnetic torques^{16,22,23,24} which add to the constant torque of the machine. These pulsating



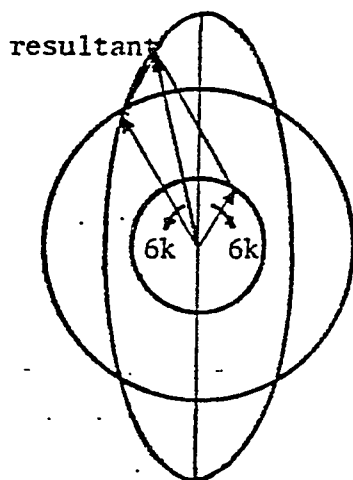
(a)

Generation of Harmonic Currents of Order $6k$ in the Rotor due to Harmonic Currents of Order $6k+1$ in the Stator.



(b)

Generation of Harmonic Currents of Order $6k$ in the Rotor due to Harmonic Currents of Order $6k-1$ in the Stator.



(c)

The Resultant Elliptical Field.

Fig. 1.1 Generation of Harmonic Currents of Order $6k$ in the Rotor

electromagnetic torques produce vibrations that could damage the machine structure, especially if their frequencies coincide with the machine natural frequencies.^{25,26}

The flow of harmonic currents in the machine windings and rotor surface increases the machine losses.^{2,3,18-21,27-30} With an increase in the losses, the machine efficiency¹⁶ is reduced and the operating cost is increased. In addition, the extra machine losses result in an increase in its temperature rise, and thus the machine should be derated^{18-20,27-30} to avoid any undue deterioration of the insulation.

This problem of the increase in the losses and heating of synchronous machines due to thyristor-bridge loading has been receiving the attention of many investigators^{18-20,27-30} for a long time. In earlier studies,^{20,29} the effort was directed towards the experimental determination of these losses and their heating effects. Few other studies^{17,18,27,28} applied approximate theoretical concepts to predict the amount of these losses by representing the synchronous machine by its negative-sequence resistance and using approximate values for the rotor harmonic currents. In all these investigations, the rotor currents were calculated by assuming that the same order harmonic currents ($6k$), which are induced in the rotor due to the one higher ($6k+1$) and the one lower order ($6k-1$) stator harmonic currents, are in phase and add together. In this context, the rotor heating effect of rectifier loads was specified^{17,18,27,28} in terms of an equivalent continuous negative-sequence current. Such a current was then compared with the generator continuous permissible negative-sequence current and reduction factors for rectifier loads were calculated. However, the results obtained from these various